1 Introduction

Alzheimer's disease (AD) is a debilitating medical condition characterised by serious and progressive cognitive decline that affects one in eight people over 65 years of age [**?**]. Alzheimer's disease is the most common dementia and appears to be due to a failure of elimination of amyloid-β (Aβ) - a normal by-product of cell metabolism - from the brain [**?**]. Precise details of the mechanism that causes AD are (largely) unknown [**?**].

Extracellular space in the brain contains interstitial fluid (ISF) which is produced by the blood and by-products of cell metabolism. The extracellular spaces within the walls of cerebral blood vessels referred to as *basement membranes* represent the perivascular pathways along which ISF drains out of the brain [**?**, **?**, **?**].

One mechanism for the removal of Aβ from the brain parenchyma is perivascular drainage, by which Aβ within ISF enters the capillary basement membranes draining to the walls of arteries towards the surface of the brain.

Figure 1: Perivascular drainage of Aβ along basement membranes.

With ageing and a certain genetic disposition soluble Aβ is not eliminated from the brain, instead it is deposited in the walls of blood vessels as *Cerebral Amyloid Angiopathy* (CAA) [**?**, **?**]. CAA may cause a blockage in the ISF drainage pathways resulting in an alteration of the composition of ISF in the brain parenchyma. This change in biochemical composition of the ISF leads to nerve cell death and Alzheimer's Disease. [**?**].

Susceptibility to CAA varies throughout the brain and vascular vessels. In particular CAA is most prominent in the occipital, temporal and frontal lobes and least prominent in the parietal lobe and the cerebellum [**?**]. We suspect that one reason for the differing unacceptability of CAA is the differing symmetry of the cerebral arterial tree. High levels of symmetry have been shown to be advantageous in other networks. For example Song *et al.* found that a fractal biochemical annotation network (a graph with a high level of symmetry) is more robust than a less symmetric graph [**?**]. In order to test the hypothesis that symmetry effects susceptibility to CAA we design and implement a graph theoretic algorithm that models CAA.

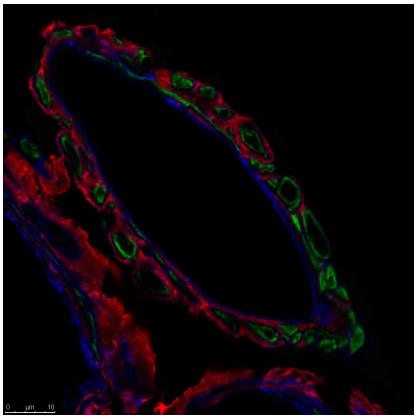

Figure 2: CAA in a cross-section of a leptomeningeal artery: the deposition of Aβ is shown in red.

2 Background

In Section **??** we will describe an algorithm that models CAA. This algorithm is constituted of two parts; a model of the anatomical structure of the perivascular drainage system and an algorithm that replicates accumulation of Aβ. We will describe this model in the language of graph theory, reformulating accumulation of Aβ as a process on a graph.

2.1 Graphs and Trees

Graph theory has a rich mathematical history dating back to Leonard Euler and more recently graph theory, under the guise of the much ballyhooed *Science of Networks*, has been applied to model diverse phenomena such as social networks, the world wide web, and the internet [**?**, **?**].

A (undirected, unweighted) graph is a pair $G = (V(G), E(G))$ such that $V(G)$ and $E(G)$ are the vertices and edges of G respectively. Every edge $e \in E(G)$ begins and ends at vertices $v, w \in V(G)$. If an edge begins and ends at the same time we call that edge a *loop*. Conversely we say that two vertices are *adjacent* if they are connected via an edge.

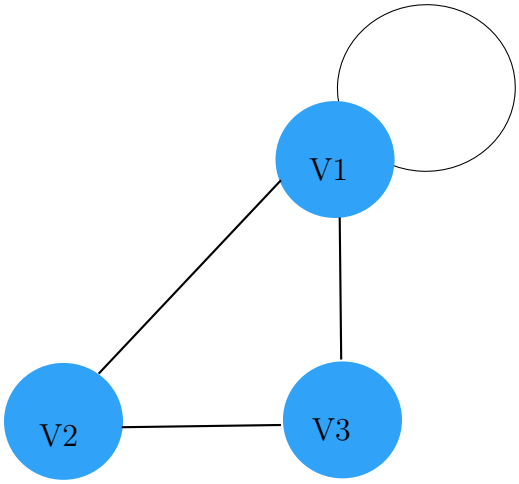

Figure 3: A graph with 3 vertices, 4 edges and 1 loop. The path 1-2-3 is a cycle

The degree, $\deg(v)$, of a vertex v is the number of edges incident to v. If $\deg(v) = 1$ then we say that v (and the edge incident to v) is a *leaf*. A path is a sequence of consecutive edges and a cycle is a path beginning and ending at the same vertex that doesn't visit an edge more than once. A *tree* is a connected graph (there exists a path between every pair of vertices) which admits no cycles or loops [**?**].

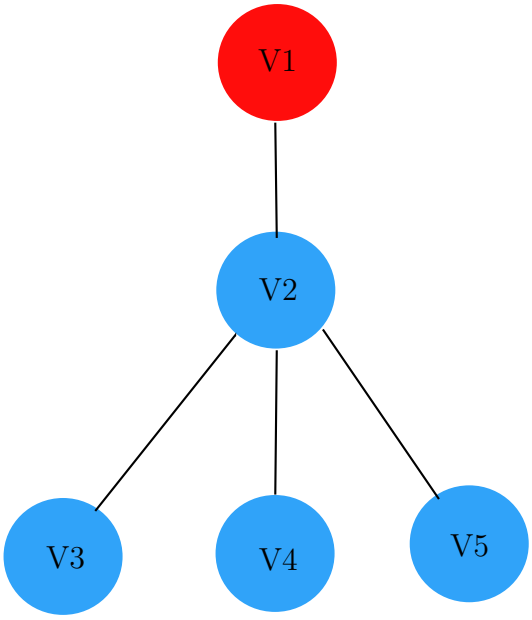

Figure 4: Tree, T with edges $\{(V1V2)(V2V3)(V2V4)(V2V5)\}$. We may permute edges $\{(V2V3)(V2V4)(V2V5)\}$ whilst preseriving adjacent vertices in 6 possible ways so $|\mathrm{Sym}(T)| = 6$. By assigning $V1$ to be the root of T notice that $\mathrm{lv}(V1) = 0, \mathrm{lv}(V2) = 1, \mathrm{lv}(V3) = \mathrm{lv}(V4) = \mathrm{lv}(V5) = 2$.. The vertices marked in blue represent an induced subtree of T, rooted at V2.

Remark. One can formally calculate the symmetry of a mathematical object such as a graph or cube by identifying that object's *group of symmetries*. For example the group of (orientation preserving) symmetries of the cube consist of all possible rotations of the cube i.e. pick the cube up, rotate it in such a way that when you put it down it will look identical to the original cube. Similarly, for a tree T the group of symmetries, $\mathrm{Sym}(T)$, consists of all permutations of vertices/edges that preserve vertex adjacency. The number of possible legal permutations is written as $|\mathrm{Sym}(T)|$ and we say that a tree with a larger number of legal permutations is more*symmetric* than a tree with a smaller symmetry group.

The vascular system comprises of a hierarchy of vessels: blood flows from arteries to arterioles to capillaries. To reflect this orientation our model will incorporate a *rooted* tree: a tree in which one vertex has been assigned the role of *root*. The *level* of each vertex $v \in V(G)$ is the length of the shortest path from the root to v, we write this as $\mathrm{lv}(v)$.

Remark. The assigned root vertex in our model will correspond to the point where Aβ drains out of the cerebral vasculature and into the lymphatic system. When we model a blockage in the perivascular system we will remove an edge from a rooted tree T which results in a failure of drainage from all vessels that flow into that edge - these vessels correspond to an *induced subtree* of T. In particular, if the edge joining vertices $v, w \in V(T)$ is removed and (without loss of generality) $\mathrm{lv}(v) < \mathrm{lv}(w)$ then we will also remove the induced subtree rooted at w from T.

Recall from Section **??** the hypothesis that there exists correlation between a high degree of symmetry and network robustness. To gain some intuition into this hypothesis consider the following (extreme) example. Let T_1 be the tree on 15 vertices depicted on the left and T_2 be the line of 15 vertices depicted on the right of Figure **??** [below]. Since $|\operatorname{Sym}(T_1)| = 128$ and that $|\operatorname{Sym}(T_2)| = 2$, T_1 is more symmetric than T_2.

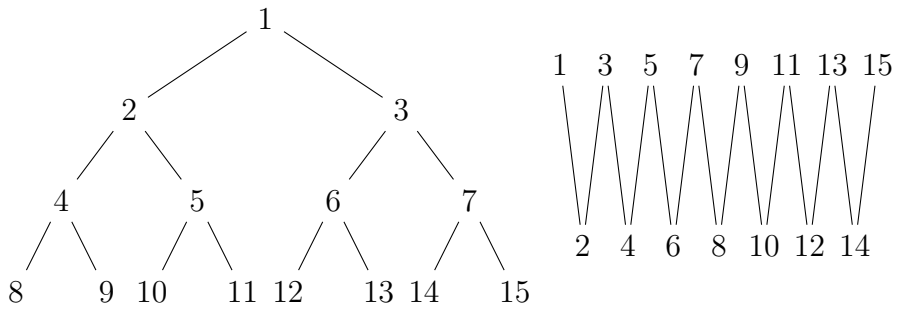

Figure 5: T_1 and T_2

If we remove an edge at random from T_1 and also remove the induced subtree adjacent to that edge the expected number of edges removed is:

$$1\frac{8}{14} + 3\frac{4}{14} + 7\frac{2}{14} = \frac{12}{7} \tag{1}$$

If we remove an edge at random from T_2 and also remove the induced subtree adjacent to that edge the expected number of edges removed is:

$$\frac{1}{14}\sum_{k=1}^{14} k = \frac{15}{2} > \frac{12}{7} \tag{2}$$

2.2 Anatomical data

In order to build an effective model of CAA we will incorporate relevant anatomical data such as arterial length, branching and the radius of vessels [1] Cassot *et al.* conducted a detailed analysis of the cerebral vasculature which has formed the basis of numerous numerical analyses [**?**, **?**, **?**]. Cassot *et al.* found that 98% of branching in the cerebral cortex is bifurcation and there are approximately 300 branching points [**?**].

At an arterial bifurcation point with parent vessel p and daughter vessels d_1 and d_2 Murray's law [**?**] states that:

$$r_p^3 = r_{d_1}^3 + r_{d_2}^3$$

where r_p is the radius of p and r_{d_1}, r_{d_2} are the radii of d_1 and d_2 respectively. Experimental evidence has shown that Murray's law is a good approximation for arterial vessels [**?**, **?**].

Murray's law describes the relationship between certain bifurcating *cylindrical vessels*, however, we will model the cerebral perivascular pathways as *annular prisms*. Therefore we will adjust Murray's law to describe the relationship between parent and child annular prisms. In addition we assume that the width of the perivascular space, ϵ, is the same for any vessel from capillary to artery. Since the notion of radius is more complicated for an annular prism we reformulate Murray's law in terms of cross-sectional area.

In addition we assume that the width of the perivascular space, ϵ is the same for any vessel from capillary to artery (the walls of cerebral capillaries consist of one fused layer of basement membrane which is approximately 150 nm in thickness). So let the parent vessel have radius $r_p = r'_p + \epsilon$ and the two daughter vessels have radii $r_{d_i} = r'_{d_i} + \epsilon$ for $i = 1, 2$.

Lemma 2.1 (Murray's law for annular prisms)**.**

$$A_p = \pi \left(\epsilon^2 + 2\epsilon \left(\left(\frac{A_{d_1} + \pi\epsilon^2}{2\epsilon\pi} \right)^3 + \left(\frac{A_{d_2} + \pi\epsilon^2}{2\epsilon\pi} \right)^3 \right)^{\frac{1}{3}} \right)$$

where A_p is the cross-sectional area of the parent vessel and A_{d_1} and A_{d_2} are the cross-sectional areas of the two daughter vessels at a bifurcation.

[1] There is a great deal of disagreement and ambiguity in the literature pertaining to arterial vessel segments and branching points [**?**]. We will use the definitions given by Cassot *et al.* [**?**]

Proof. The relationship between the cross-sectional area, A_X of any vessel and the radius, r_X of that vessel is given by the formulae:

$$\begin{aligned} A_X &= \pi((r'_X + \epsilon)^2 - r'^2_X) \\ &= \pi(\epsilon^2 + 2\epsilon r'_X) \\ r'_X &= \frac{A_X - \pi\epsilon^2}{2\epsilon\pi} \\ r_X &= \frac{A_X - \pi\epsilon^2}{2\epsilon\pi} + \epsilon \\ &= \frac{A_X + \pi\epsilon^2}{2\epsilon\pi} \end{aligned}$$

By combining the above equations we find that the cross-sectional area of the parent vessel, A_p, is given by:

$$\begin{aligned} A_p &= \pi(\epsilon^2 + 2\epsilon r_p) \\ &= \pi\left(\epsilon^2 + 2\epsilon(r_{d_1}^3 + r_{d_2}^3)^{\frac{1}{3}}\right) \\ &= \pi\left(\epsilon^2 + 2\epsilon\left(\left(\frac{A_{d_1} + \pi\epsilon^2}{2\epsilon\pi}\right)^3 + \left(\frac{A_{d_2} + \pi\epsilon^2}{2\epsilon\pi}\right)^3\right)^{\frac{1}{3}}\right) \end{aligned}$$

□

3 Method

In this section we will describe the algorithm we designed to replicate CAA [2]. This algorithm has three constituent parts:

(i) Generate 50 random rooted binary (each vertex has degree less than 4) trees $\mathcal{T} = \{T_1, T_2, \ldots, T_{50}\}$.

(ii) Calculate the order of the symmetry group of each tree using the graph isomorphism program *nauty* [**?**].

(iii) Replicate CAA by removing edges $e \in E(T_i)$.

[2]This algorithm was implemented using the numerical modelling program *matlab* [**?**]

In accordance with the anatomical survey paper by Cassot *et al.* discussed in Section **??** each rooted binary tree was generated with 300 vertices. Each edge $e \in E(T_i)$ was associated with an annular prism and assigned a volume $\mathrm{vol}(e)$. Leaf edges were defined to have volume 1 and subsequent edges were given a volume consistent with Murray's law for annular prisms. The *initial* volume of each tree T_i was defined to be

$$\mathrm{Vol}(T_i) = \sum_{e \in E(T_i)} \mathrm{vol}(e)$$

The process of edge removal proceeds as follows: at time $t = 0$ we set $T_i(0) = T_i$ (our randomly generated rooted binary tree). At subsequent times $t = 1, 2, \ldots$ we associated a probability $0 < P_t \leq 1$, that edge e was to be removed at time t, with every edge $e \in E(T(t))$. If edge e was removed then the induced subtree rooted at the endpoint of e greatest distance from the root of T_i was also removed to form $T_i(t)$.

The volume of T_i at time t was defined to be $\mathrm{Vol}_t(T_i) = \sum_{e \in E(T_i(t))} \mathrm{vol}(e)$. We then defined concentration:

$$C(t) = \frac{\mathrm{Vol}(T_i}{\mathrm{Vol}_t(T_i)}.$$

We can now define

$$P_t = \begin{cases} p.C(t) & \text{if } p.C(t) < 1 \\ 1 & \text{otherwise} \end{cases} \quad \text{where } 0 < p < 1$$

Finally, we recorded the time, τ_i, taken to remove half of the edges from each T_i (henceforth we will refer to τ_i as the *half-life*).

4 Results

For each tree T_i we calculated the order of the symmetry group $|\mathrm{Sym}(T_i)|$ and the minimum time, τ_i, taken for at least half of the edges $e \in E(T_i)$ to be removed from T_i. We further calculated the median order of symmetry group, $\phi =$, and partitioned $\mathcal{T}$ into two subsets as follows:

$$\mathcal{T}_1 = \{T_i \in \mathcal{T} : |\mathrm{Sym}(T_i)| < \phi\} \text{ and } \mathcal{T}_2 = \{T_i \in \mathcal{T} : |\mathrm{Sym}(T_i)| < geq\phi\}$$

We also calculated the mean values, μ_j $(j = 1, 2)$ of τ_i for trees in $\mathcal{T}_j$ for $j = 1, 2$:

$$\mu_j = \frac{\sum_{T_i \in \mathcal{T}_j}}{|\mathcal{T}_j|}$$

Figure **??** shows the μ_j corresponding to the $\mathcal{T}_j$

half.jpeg

Figure 6: Mean time for $\frac{1}{2}$ edges to be removed for high and low values of $|\operatorname{Sym}(T_i)|$

It is clear that the trees with a larger symmetry group had a much greater mean half-life.

4.1 Discussion

In order to place our results back into a medical context recall that the edges and vertices of each tree T_i correspond to arterial vessels and branching points respectively. The half-life, τ_i associated with each tree describes the rate at which drainage pathways become obstructed i.e. the rapidity of the onset of CAA.

In order to build an effective model of CAA it was necessary to make several simplifying assumptions. We defined the probability that an edge was removed in terms of the concentration of Aβ but the distribution of deposition of Aβ in a real arterial vessel is complex and not fully understood [**?**]. Similarly, our model of CAA was discrete, i.e. an edge either allowed free flow of ISF or was blocked but in reality CAA is a gradual process. In a future model of CAA we would recommend variable edge flow. Ambrose has shown that the brain undergoes angiogenisis which could be reflected by including a new random parameter which governs the introduction of edges in our algorithm [**?**]. Modelling basement membranes as annular prisms does not take into account the tortuous routes of perivascular drainage therefore one might also include a tortuosity parameter in a more refined model. Finally, we could model arteriosclerosis (suspected to be a major contributing factor to CAA [**?**, **?**]) by introducing a monotonically decreasing radial function.

Our results suggest that a more symmetric cerebral arterial tree could indicate a higher degree of robustness to CAA, however we stress that ours is a very rudimentary model. Further evidence of this correlation could be found by experiment examining the relationship between highly symmetric areas of the brain and the extent to which those areas are affected by CAA.

5 Conclusion and Clinical Implications

We have demonstrated that it is likely that there is correlation between symmetry of the cerebral vasculartureand lower risk of proliferation of CAA.